minerals

MDPI

Article

Geochemical Reconstruction of the Provenance, Tectonic Setting and Paleoweathering of Lower Paleozoic Black Shales from Northern Europe

Sylvester Ofili [1,*], Alvar Soesoo [1,2], Elena G. Panova [3], Rutt Hints [2], Sigrid Hade [2] and Leho Ainsaar [1]

[1] Department of Geology, Institute of Ecology and Earth Sciences, University of Tartu, Ravila 14a, 50411 Tartu, Estonia; alvar.soesoo@ut.ee (A.S.); leho.ainsaar@ut.ee (L.A.)
[2] Department of Geology, Tallinn University of Technology, Ehitajate tee 5, 19086 Tallinn, Estonia; rutt.hints@taltech.ee (R.H.); sigrid.hade@taltech.ee (S.H.)
[3] Department of Geochemistry, Saint Petersburg State University, University Embankment, 7/9, Saint Petersburg 199036, Russia; e.panova@spbu.ru
* Correspondence: sylvester.ofili@ut.ee

Abstract: Lower Paleozoic black shales from Estonia, Sweden, and Russia were analyzed for major and trace elements to reconstruct the provenance, tectonic setting, and paleoweathering conditions of these shales. The black shale is highly enriched in U, V, Mo, and Pb (except in samples from Sweden where Pb is slightly enriched), slightly enriched in SiO_2, Fe_2O_3, K_2O, and TiO_2 and highly depleted in CaO, Na_2O, and MnO, with respect to average shales. The provenance signatures (Th/Sc versus Zr/Sc, Al_2O_3 versus TiO_2, Zr versus TiO_2 plots, and Zr/Sc ratio) of the Baltoscandian black shales suggest that they were derived from rocks of intermediate to felsic composition and from recycled sediments. The likely provenance region was the Paleoproterozoic igneous and metamorphic basement of southern central and southern Finland, which consists predominantly of felsic to intermediate metamorphic (acidic to intermediate gneisses, felsic volcanics, microcline granites and migmatites) and igneous rocks (small granitic intrusions and large rapakivi granite intrusions), and reworked older Ediacaran and Lower Cambrian sediments; however, the proportion of clastic input from these sources is not uniform in the three regions studied. The discrimination of the tectonic settings of source materials of the black shale using the SiO_2 versus K_2O/Na_2O plot and a new discriminant method (APMdisc) favors a passive margin setting. The Chemical Index of Weathering (CIW) indicates that the clastic material in the black shale of the studied regions has experienced an intense degree of chemical weathering. Weathering indices (Chemical Index of Alteration CIA and CIW) also show that the black shale has experienced significant secondary potassium enrichment.

Keywords: black shale; graptolite argillite; alum shale; Dictyonema shale; provenance; tectonic setting; paleoweathering

check for updates

Citation: Ofili, S.; Soesoo, A.; Panova, E.G.; Hints, R.; Hade, S.; Ainsaar, L. Geochemical Reconstruction of the Provenance, Tectonic Setting and Paleoweathering of Lower Paleozoic Black Shales from Northern Europe. *Minerals* **2022**, *12*, 602. https://doi.org/10.3390/min12050602

Academic Editor: Luca Aldega

Received: 10 March 2022
Accepted: 6 May 2022
Published: 10 May 2022

Publisher's Note: MDPI stays neutral with regard to jurisdictional claims in published maps and institutional affiliations.

Copyright: © 2022 by the authors. Licensee MDPI, Basel, Switzerland. This article is an open access article distributed under the terms and conditions of the Creative Commons Attribution (CC BY) license (https://creativecommons.org/licenses/by/4.0/).

1. Introduction

The major and trace element composition of marine siliciclastic and mixed organic-siliciclastic sedimentary rocks is dependent on several variables including tectonic setting, weathering, and sediment provenance [1,2]. It is therefore possible to infer these variables for a suit of clastic rock by studying its geochemical fingerprints. This approach has been known for a long time. Some pioneering geochemical studies established the relationship between the geochemical composition and tectonic setting of siliciclastic rocks [1,3,4]. In furtherance of knowledge, the authors of [5,6] extended this relationship to include sediment provenance and weathering. Verma and Armstrong Altrin [7] developed a new method of tectonic setting discrimination. Numerous studies have shown the applicability of these geochemical proxies in constraining the provenance, tectonic setting, and degree

of weathering of sedimentary rocks [8–10]; however, care should be taken when making interpretations because of a possible complex interplay of variables, which can significantly affect the authigenic fractions of the chemical elements in clastic rocks [11,12].

Cambro–Ordovician fine-grained black shales are widespread in the Baltoscandian region (Figure 1). They extend from Norway through Denmark, Sweden, Poland, Lithuania, Latvia, and Estonia to western Russia [13]. These metalliferous black shales are commonly highly enriched in U, V, and Mo [14–18]. In Sweden, the U content of the black shale (Alum shale) regularly reaches up to 300 ppm [19], and in exceptional instances, up to 6000 ppm in some specific organic-rich intervals [20]. The maximum total thickness of the Cambrian and Tremadocian black shale sequence is 178 m along the Danish coast, decreasing to 20–25 m in stratigraphically less complete sequences in central Sweden [21,22]. The thickness progressively decreases further eastward, to a maximum of 7.4 m in Estonia and 6 m in Russia [18,23]. The U, V, and Mo contents of the black shale in Estonia (Graptolite Argillite) reach 1200, 1600, and 1000 ppm, respectively [24]. The black shale (Dictyonema Shale) in Russia has V and Mo concentrations up to 900 and 200 ppm, respectively [23]. This significant metal enrichment makes the Cambro–Ordovician black shale of Baltoscandia a potential future source of raw material for Europe.

However, the source of the metals and their distribution in the black shale is still up for debate. Recent studies have shown that the geochemical composition of the black shale is laterally and vertically heterogenous [18,19,23,24]. This pronounced variation could be a consequence of several factors, including variation in primary clastic input and changing depositional environmental conditions.

Although most of the paleoenvironmental geochemical studies concentrate on syngenetically enriched metal assemblages, the variance of the primary clastic material is much less studied, and the influence of clastic fractions on the cumulative trace element pool of the considered black shale remains poorly understood. The erosion and re-deposition of the older Ediacaran and Lower Cambrian sediments, input of volcanic ash, and reworking of material from Proterozoic metamorphic, igneous, and volcanogenic assemblages have been suggested as major clastic sources of the Upper Cambrian–Tremadocian sediments in the Baltic Paleobasin [25–28]. Some studies, for example Schultz et al. [29] indicate that the input of the clastic fraction may have significantly influenced the variability of trace element abundance in the black shales.

In this study, we present a detailed major and trace element geochemical characterization of black shale samples from Sweden, Estonia, and Russia. The geochemical fingerprints are applied to infer the provenance, tectonic setting, and degree of chemical weathering of the clastic fraction of the black shale.

2. Geological Background

The Baltic Paleobasin was a long-lived epicontinental basin which existed during the Cambrian–Silurian period on the Baltica paleocontinent and was surrounded by the Fennoscandian and Sarmatian oldlands. The Cambrian sediments of the considered region generally lie unconformably upon the Paleoproterozoic gneisses and plutonic granites, representing a transgression which started in the late Neoproterozoic era [30]. The shallow and flat-bottomed Baltic Paleobasin flooded extensive areas on the low-lying peneplained and tectonically stable continent in the Cambrian and Early Ordovician periods, including large marginal areas of the Fennoscandian Shield [31]. This period was characterized by a globally high sea-level, a likely occurrence of a global-scale ocean anoxic event, and episodes of the accumulation of organic-rich sediments in all paleocontinents [17,32]. Furthermore, $\delta^{18}O$ studies suggest that the Cambrian–Tremadocian transition might have experienced exceptionally high global paleotemperatures [33], although the Baltica paleocontinent was situated well southward from the tropical paleolatitudes [30].

In the middle Cambrian period, the isolated Baltica paleocontinent was located at high southern latitudes and drifted northward, reaching high middle latitudes during the Early Ordovician period. The drift was accompanied by fast anti-clockwise rotation of

the continent [30]. At the start of the Ordovician period, the Baltoscandian part of the paleocontinent was largely covered by the Baltic Paleobasin, which faced the Iapetus Ocean in the western margin of Baltica [34].

During the late Cambrian to early Ordovician periods, black shales were widespread in the Baltic Paleobasin (Figures 1 and 2). They were deposited in a large shallow epicontinental sea that covered substantial parts of Baltica at maximum sea level stand [16]. Black shale deposition in Estonia and Russia has been placed within the shallowest areas of the epicontinental sea [16]. In Estonia, they consist of dark brown organic-rich mudstone that was deposited in the Early Ordovician period [35,36]. They represent the Türisalu Formation [15], varying in thickness from about 0.5 m in the southern and eastern regions to a maximum of 7 m in the NW region [18]. Anthraconite concretions and disseminated pyrite are common features of this black shale.

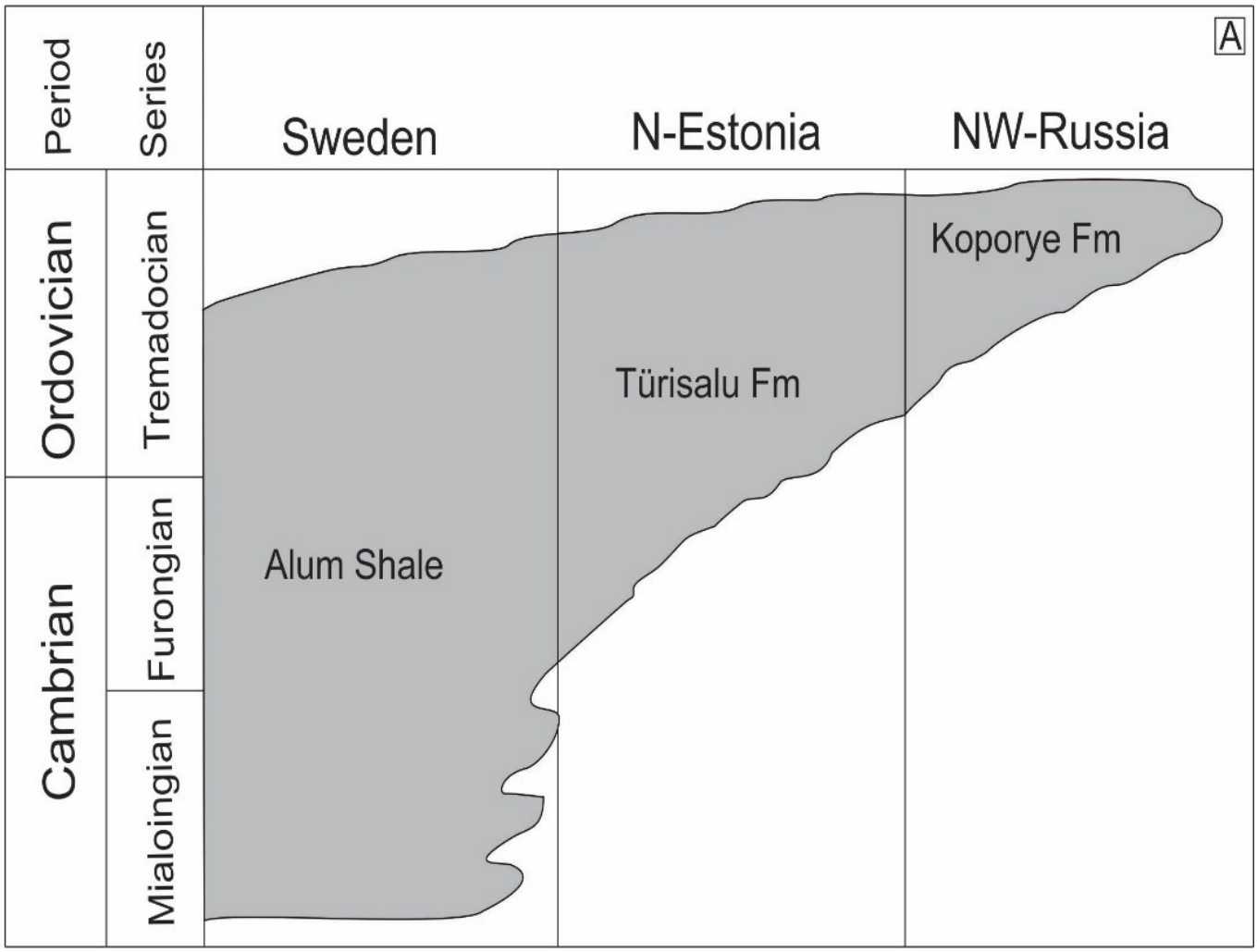

Figure 1. *Cont.*

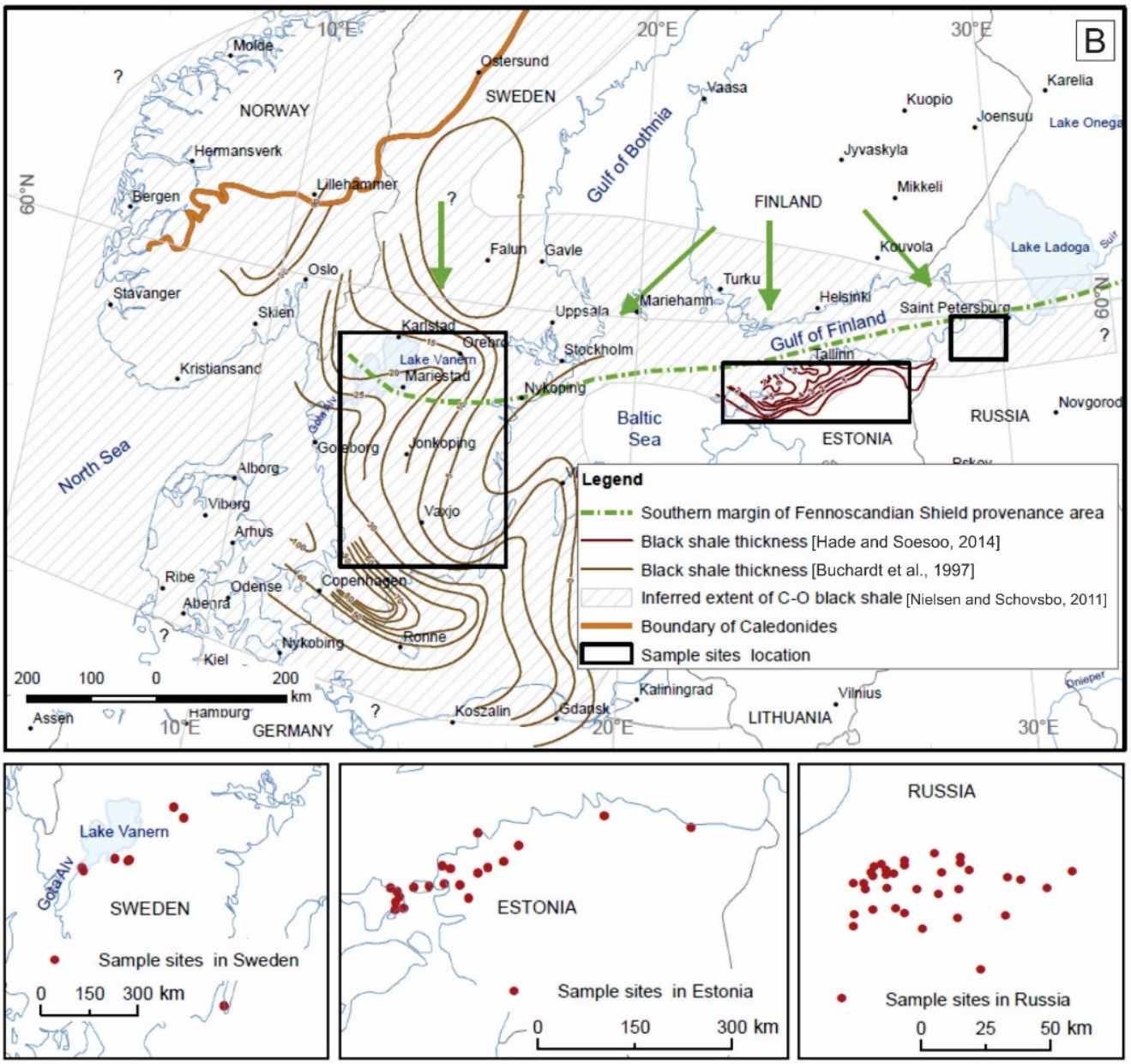

Figure 1. (**A**) Simplified stratigraphy of black shale in the Baltic Paleobasin after [21,37]. (**B**) Map of black shale areas showing sampling points after [24,38,39]. The green arrows represent possible directions of sediment provenance, while dotted green lines represent the southern Fennoscandian landmass between the middle Cambrian to middle Ordovician periods, constructed according to [40], regarding the tectonophysics for those periods. Question mark represents uncertainty in black shale distribution.

Ordovician sediments representing the entire Ordovician sequence are also common in most of the Leningrad region. The lower Ordovician includes the Tosna and Koporye Formations. The Koporye Formation is the lateral equivalent of the Türisalu Formation in Estonia. The lower part of the Koporye Formation is composed of overlapping fine-grained sandstones and black kerogenic mudstones, with a thickness of 2–15 cm. In some places, mudstone is replaced by shaley bituminous clays containing graptolite remains.

In the territory of Sweden, the black shale Formation belongs to the Middle Cambrian–Early Ordovician time interval [41]. This Formation is commonly called Alum Shale because historical raw materials for the production of alum were extracted from this shale.

The upper part of the Early Cambrian sand Formation is composed of glauconitic sandstone which is overlain by gray-green siltstones and shale of Middle Cambrian age. The rocks are separated by a thin layer of conglomerates. The Middle Cambrian facies of black shale of the Alum Shale Formation lies higher in the section.

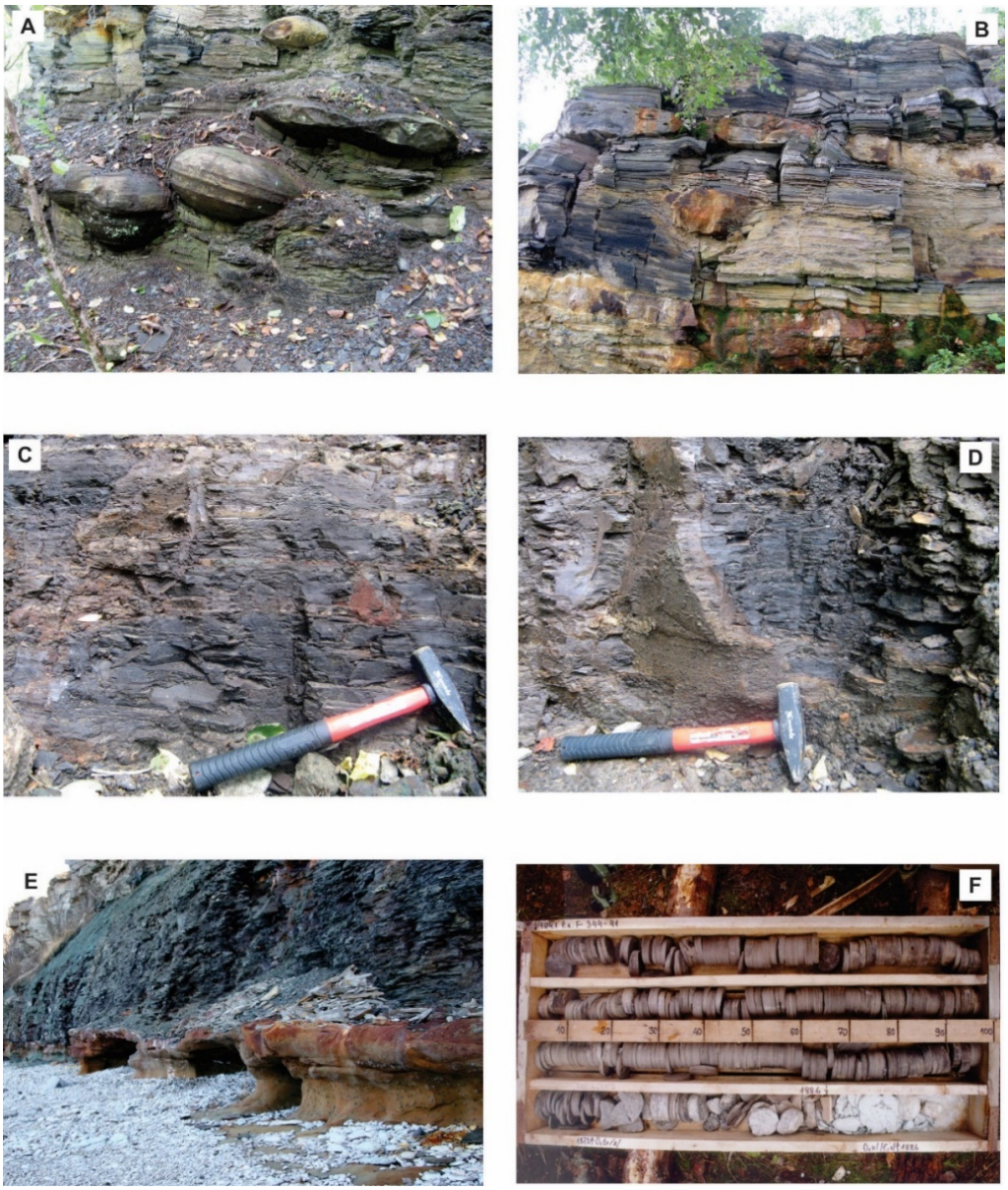

Figure 2. Representative outcrop and drill core photographs of the studied black shale. (**A**,**B**) Outcrops in Billingen and Kinnekulle, Sweden; (**C**,**D**) outcrops in western Russia; (**E**,**F**) outcrop in the Pakri Peninsula (NE Estonia) and drill core F344 (W Estonia), respectively.

3. Materials and Methods

A total of ten drill cores (F298, F330, F343, F344, F369, F362, F355, K14, F366, F354) from the drill core repository of the Geological Survey of Estonia were studied to characterize the Estonian part of the black shale. The samples were taken at 20 cm intervals where possible. For some thin beds, the sampling interval was 10 cm or less, whereas intervals greater than 20 cm were used in sections with very poor recovery. The chemical composition of samples was analyzed by the Rigaku wavelength dispersive X-ray fluorescence spectrometer ZSX Primus II (manufactured by Rigaku, USA), and 3 kW Rh primary radiation was used to measure the concentrations of elements. For calculations, the semi-quantitative SQX

Analysis software (version 3.44) was used. Trace element analysis was carried out on selected samples from six drill cores (F369, F362, F355, K14, F366, F354) at Bureau Veritas, Canada, using the procedure with code MA250. For this procedure, a 0.25 g split was heated in HNO_3, $HClO_4$, and HF for fuming and then taken for drying. The residue was thereafter dissolved in HCl. The trace element data for the remaining four drill cores (F298, F330, F343, F344), and major and trace element data for additional seven drill cores (F314, F326, F328, F338, F345, F347, F360) and one outcrop (Nõmmeveski), were collected from the report of the Geological Survey of Estonia [42] and from [43] (Tables 1 and 2 and Supplementary Table S1). Geochemical data from two outcrops (Pakri and Saka, [18]) were also included in this study (all analyses in the Supplementary Data). The drill cores of graptolite argillite are mostly available from north-western Estonia where the argillite is the thickest. The thickness of the studied cores ranges from 0.3 to 6.7 m. In terms of mineralization, pyrite and glendonites are often observed in these drill cores. In places, the black shale beds are interrupted by lenses of sandstone. The black shale complex covers light gray sandstones of the Kallavere Formation, which, in some places, contains abundant phosphatic brachiopod shells.

Table 1. Average major element concentrations (in wt%) of representative black shale drill cores in Estonia and Russia, and outcrops in Sweden.

Sample	Latitude	Longitude	SiO_2	Al_2O_3	Fe_2O_3	MnO	CaO	MgO	Na_2O	K_2O	TiO_2	P_2O_5
Estonia												
F298	59.297927	24.597908	48.50	12.51	4.51	0.02	0.54	1.11	0.17	6.53	0.59	0.21
F330	59.1524027	23.540536	46.74	12.21	4.32	0.02	0.47	1.01	0.22	6.52	0.58	0.12
F343	59.007919	23.356647	46.17	12.42	4.18	0.02	0.32	1.10	0.21	6.35	0.58	0.17
F344	58.9189	23.903258	43.99	11.78	4.63	0.03	2.02	2.01	0.17	6.12	0.55	0.20
Sweden												
Kvantorp	59.119473	15.284068	53.77	8.67	3.72	0.01	0.40	0.58	0.12	3.25	0.34	0.07
Latorp	59.277967	15.008981	51.40	8.49	4.11	0.01	0.21	0.55	0.16	3.45	0.40	0.08
Kinnekule	58.538663	13.36666	53.70	10.50	4.23	0.01	0.28	1.87	0.15	3.27	0.88	0.08
Billingen	58.505331	13.739959	52.83	13.58	7.49	0.01	0.20	1.74	0.19	3.94	0.89	0.09
Russia												
1	59.705477	29.043983	68.60	8.96	5.67	0.04	2.35	1.12	0.13	5.39	0.62	0.51
4	59.6525861	29.0467861	58.97	8.36	5.38	0.02	1.81	0.88	0.11	4.92	0.53	0.50
5	59.6309389	29.0434333	52.82	8.33	6.86	0.03	2.12	1.04	0.11	4.85	0.51	0.50
11	59.7363167	29.1151028	58.26	9.22	4.49	0.02	1.39	0.80	0.11	5.41	0.53	0.32

Major and trace element data from outcrops in eight districts in southern Sweden and 34 drill cores from western Russia [44] were also collected and utilized for this study to represent the Swedish and Russian parts of the black shale regions (Tables 1 and 2 and Supplementary Materials). In most outcrops of Sweden, the Upper Cambrian interval of the black shale was sampled layer by layer from the bottom upward. Only in Billingen section, was the Middle Cambrian interval sampled in addition to the Upper Cambrian interval. Great care was taken to ensure that only fresh, unweathered samples were collected for laboratory studies. The intervals containing carbonate nodules were not selected.

The trace element contents of the samples were studied using the Inductively Coupled Plasma-Mass Spectrometry. Prior to analysis, the samples were crushed to a grain size of 74 μm. Nitric, hydrochloric, and hydrofluoric acids of high purity, additionally purified by distillation, as well as deionized water, were used to decompose the samples and dissolve the salts. The analysis of the prepared solutions was carried out on Agilent 7700 and ELAN-6100 DRC devices at the Russian Geological Research Institute (VSEGEI), St. Petersburg. Major element concentration was studied using the Rigaku Miniflex II X-ray fluorescence spectrometer.

Table 2. Average trace element concentrations (in ppm) of representative black shale drill cores in Estonia and Russia, and outcrops in Sweden.

Sample	Latitude	Longitude	Ba	Cu	Mo	Ni	Pb	Sc	Sr	Th	U	V	Zn	Zr
Estonia														
F298	59.29793	24.59791	361.30	102.05	82.42	93.33	97.37	11.66	68.30	12.63	58.56	647.83	65.35	111.03
F330	59.1524	23.54054	367.65	88.39	194.35	114.36	121.31	11.16	74.06	12.14	96.45	1003.35	65.74	114.93
F343	59.00792	23.35665	370.00	112.28	183.95	173.35	143.93	11.47	76.85	12.68	124.32	1209.75	198.60	110.92
F344	58.9189	23.90326	325.65	99.40	193.80	146.78	113.47	11.21	78.37	12.65	118.90	999.39	88.65	106.39
Sweden														
Kvantorp	59.11947	15.28407	316.33	45.08	146.00	42.91	37.22	6.69	60.59	6.25	80.22	390.22	39.42	85.73
Latorp	59.27797	15.00898	322.33	64.44	163.74	44.34	31.88	7.33	51.56	7.66	121.31	441.78	66.24	91.78
Kinnekule	58.53866	13.36666	600.80	25.54	176.20	24.38	28.76	8.85	97.91	7.25	60.77	841.20	51.17	118.84
Billingen	58.50533	13.73996	634.15	95.05	209.04	73.35	42.82	12.39	56.96	10.89	97.00	695.69	90.17	153.69
Russia														
1	59.70548	29.04398	396.67	81.28	81.65	77.99	104.30	6.16	90.31	10.18	104.83	472.06	32.46	177.67
4	59.65259	29.04679	328.33	90.93	172.30	133.54	104.11	8.32	63.84	11.40	173.42	593.44	951.03	166.56
5	59.63094	29.04343	330.17	83.40	175.55	151.92	77.78	9.09	61.08	11.26	174.13	681.00	1518.19	158.00
11	59.73632	29.1151	365.67	82.57	157.30	135.55	99.87	9.15	51.42	11.05	240.27	761.83	463.43	138.33

4. Results

4.1. Major Elements

Major element data for this study are presented in Table 1 and in Supplementary Data. The most abundant major elements in the black shale are SiO_2, Al_2O_3, Fe_2O_3, and K_2O, in decreasing order of abundance. Samples from Russia had the highest concentration of SiO_2 ranging from 37 to 84 wt%, with an average value of 58 wt%. It also shows the corresponding lowest Al_2O_3 content, indicating that Al_2O_3 is associated with the finer fractions.

In Estonia, the SiO_2 content ranges from 12 to 72 wt%, with the average being 47 wt%. Only three samples had values less than 35 wt%. The SiO_2 contents in samples from Sweden are lower than in those from Russia, but slightly higher than in samples from Estonia. The average SiO_2 concentration in samples from Sweden is 52 wt%.

When compared with Post Archean Australian Shale, PAAS [45], the black shale is slightly enriched in SiO_2, Fe_2O_3, K_2O, and TiO_2, and highly depleted in CaO, Na_2O, and MnO in all studied sites (Figure 3). The positive correlation between K_2O and TiO_2 with Al_2O_3 (0.76 and 0.83, respectively) indicates that the distribution of these elements in the black shale is likely controlled by the primary input of fine-grained clastic material to the organic-rich sediment. A negative correlation exists between Al_2O_3 and CaO, possibly suggesting that the majority of CaO occurs in the calcite phase, whereas Al_2O_3 is related to the clay fraction.

4.2. Trace Elements

The average trace element values of samples from four drill cores from Estonia, Russia and outcrops from Sweden are given in Table 2. The complete data set is given in the Supplementary Materials. Post Archean Australian Shale normalized data show that the samples are highly enriched in U, V, and Mo (Figure 3). Pb is also highly enriched in samples from Estonia and Russia but slightly enriched in Swedish samples. Black shale samples show a 10-fold enrichment in Zn in samples from Russia, a 3-fold Zn enrichment in Estonian samples, and a depletion in samples from Sweden, relative to average shales (Figure 3). The Mo concentration varies widely, being 2–562 ppm in Russia, 6–1844 ppm in Estonia, and 2–411 ppm in Sweden. The average Mo concentrations are 189, 175 and 142 ppm for samples from Estonia, Sweden, and Russia, respectively. The content of U is the lowest in the Swedish samples, with an average value of 82 ppm, but twice as

high in samples from Russia, with an average value of 169 ppm. In Estonia, the average U concentration is 105 ppm. Few samples show unusually low concentrations of U, V, and Mo, likely due to the presence of sand lenses in some sections of the black shale bed.

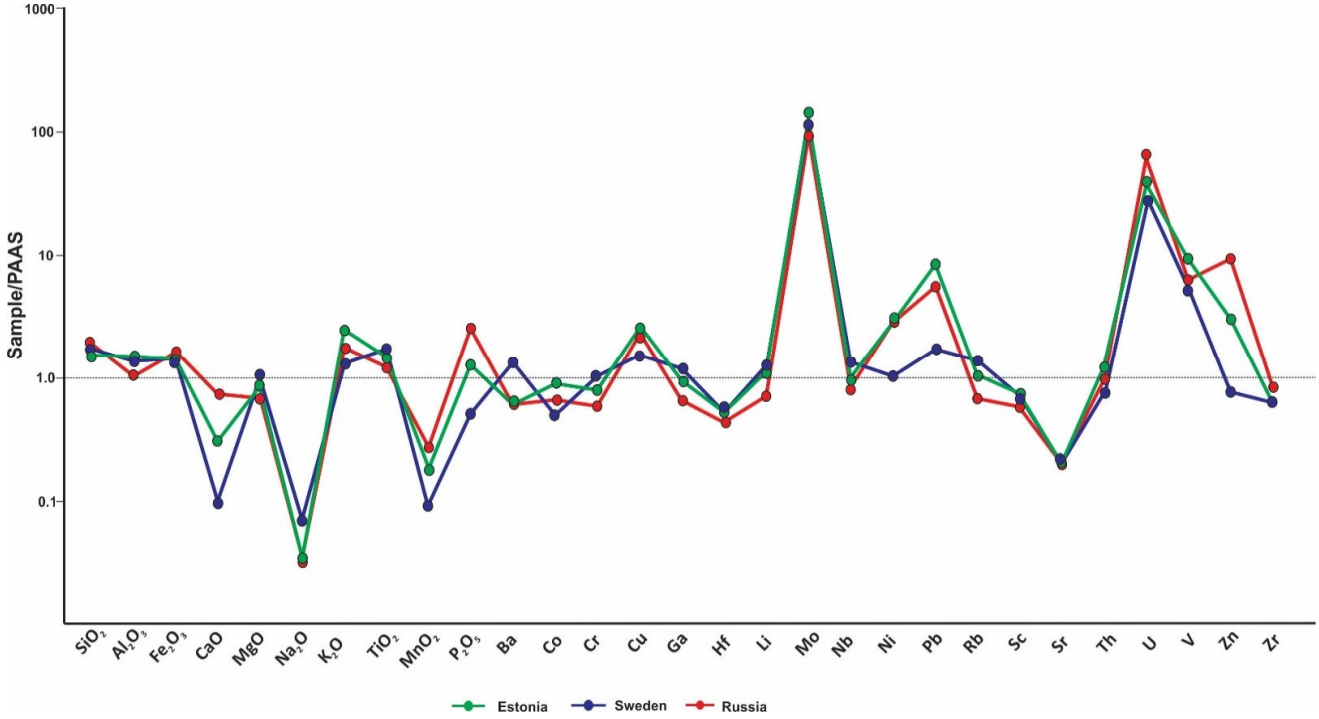

Figure 3. Major and trace element concentrations normalized against Post Archean Australian Shale [45]. The lines represent average elemental concentrations of drill cores from Estonia and Russia, and outcrops from Sweden.

5. Discussion

5.1. Provenance

Due to the relatively immobile behavior of certain trace elements under surface weathering conditions, they can be transferred from parent rock to sediment without a significant gain or loss in concentration during processes leading to deposition [46]. Nevertheless, the fractionation and recycling of clastic material may affect provenance interpretations, which were made using immobile elements [46,47]. Nevertheless, immobile elements are extensively used for the characterization of the provenance of sedimentary rocks. Some trace elements such as La and Th are mostly concentrated in felsic rocks, whereas Sc, Cr and Ni are found more frequently in basic rocks [48]; therefore, their ratios can provide information about the possible sediment sources for deposited sediments. The Th/Sc versus Zr/Sc plot (Figure 4A) was used to infer the provenance of the black shale in Sweden, Estonia, and Russia [46]. The samples from the Sweden plot in the felsic field suggest that felsic rock may be the dominating source of the sediments. Samples from Estonia and Russia plot also contain felsic rock, but they exhibit a trend in the direction of Zr addition. This may indicate that the provenance of samples from Estonia and Russia is composed of a mix of felsic rocks and recycled sediments. This interpretation is corroborated by the relatively higher ratios of Zr/Sc and K_2O/Na_2O in Russian and Estonian samples (respective average values 23 and 13 for Zr/Sc and 48 and 77 for K_2O/Na_2O).

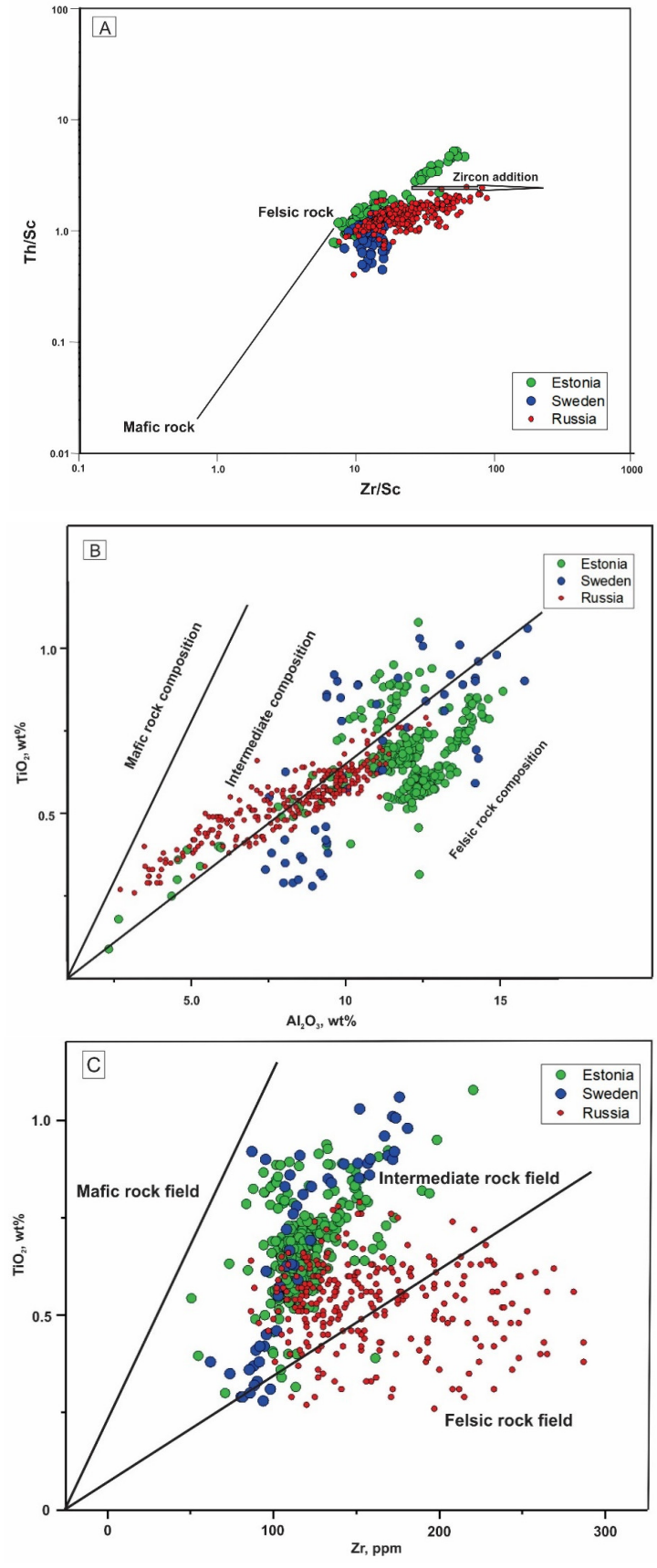

Figure 4. Provenance discrimination diagrams: (**A**) Th/Sc versus Zr/Sc [46]; (**B**) TiO_2 versus Al_2O_3; (**C**) TiO_2 versus Zr [2].

Cambrian–Ordovician reconstructions by [38,49–52] show that continental landmasses existed in the north and north-west of the black shale area. Thus, the likely provenance region for the studied black shales was the Paleoproterozoic igneous and metamorphic basement of southern Central and Southern Finland. Those rocks consist predominantly of felsic to intermediate metamorphic (acidic to intermediate gneisses, felsic volcanics, microcline granites and migmatites) and igneous rocks (small granitic intrusions and large rapakivi granite intrusions). A good representation of these rocks and the rock variation is the Central Finland Granitoid Complex with a north–south and west–east expanse of more than 200 km. Some mafic igneous intrusions and metamorphic rocks of intermediate to basic composition (mafic metavolcanics, metasediments–gneisses) are also found in this area ([53], and references therein).

The Al_2O_3 versus TiO_2 ratios have been widely applied in provenance studies. The ratios 3–8, 8–21 and 21–70 are interpreted as suggesting mafic, intermediate, and felsic sources, respectively [2]. The ratios for the studied samples are in the range of 9–39, with average values of 17, 18, and 15 for samples from Sweden, Estonia, and Russia, respectively (Figure 4B). These data suggest that the studied black shales are derived from a mix of rocks of felsic and intermediate composition.

The interpretation of the Zr versus TiO_2 plot [2] also agrees with a felsic to intermediate provenance for the black shale (Figure 4C). In this plot, samples from Sweden and Estonia fall almost entirely in the intermediate rock field (except for six samples in the felsic rock field). Samples from Russia, however, plot in both intermediate and felsic provenance fields.

According to Bhatia and Crook [1], the concentration of SiO_2 increases with a decrease in TiO_2, MnO, CaO, MgO, Al_2O_3, and Na_2O due to an increase in quartz content as a response to a change in provenance from mafic to felsic rock. There is also a significant increase in the enrichment of elements with highly charged cations (Th, U, Nb, Zr) from mafic to felsic provenance. Among the studied samples, black shales from Russia have the highest average SiO_2 content of 58.4 wt%, and correspondingly the lowest average contents (in wt%) of TiO_2 (0.53), MgO (0.95), Al_2O_3 (8.17), and Na_2O (0.10). The samples from Russia show also a significantly higher enrichment of Zr and U. Estonian samples have the lowest SiO_2 content of 47 wt% and the highest content of Al_2O_3 (12 wt%). The compositional variations in the studied samples may be related to the provenance of the clastic fraction of the black shale, with samples from Russia receiving the most felsic detrital input.

Bhatia and Crook [1] also noted a decrease in V and Sc concentrations from mafic to felsic rock. The V and Sc average concentrations of the studied samples are 972 and 10.48 ppm for Estonia, 578 and 9.72 for Sweden and 666 and 7.8 for Russia. This generally agrees with a more felsic source contribution in Russian samples compared with those from Estonia and Sweden. The studied major and trace element contents and ratios display the heterogeneity of rock types in Southern and south-central Finland well. More felsic provenance for Russian samples may be attributed to the vicinity of a large rapakivi granite intrusion (Vyborg pluton) in south-eastern Finland, which is a major sediment transport source for the black shale area in Russia.

5.2. Tectonic Setting

The chemistry of sedimentary rocks could be used as a fingerprint for inferring the tectonic setting of derived sedimentary material. One of the most widely used tectonic setting discrimination methods is the approach by Roser and Korsch [3]. It is based on the premise that the SiO_2 content and K_2O/Na_2O ratio significantly differ from one tectonic setting to another. The $\log(K_2O/Na_2O)$ versus SiO_2 plot for tectonic discrimination has been used by numerous authors [6,54,55].

The studied black shale samples generally suggest a passive margin tectonic setting (Figure 5A). All samples from the Russian plot are in the passive margin field, suggesting that the tectonic setting during deposition was entirely a passive margin. Samples from Estonia closely follow this trend, with only about 6 out of 362 samples plotting in the active continental margin. Samples from Sweden cluster around the boundary between the

passive margin and the active continental margin, with fewer samples plotting in the active continental margin field. This pattern also suggests sediments are generally derived from a passive margin for the Swedish Alum shale.

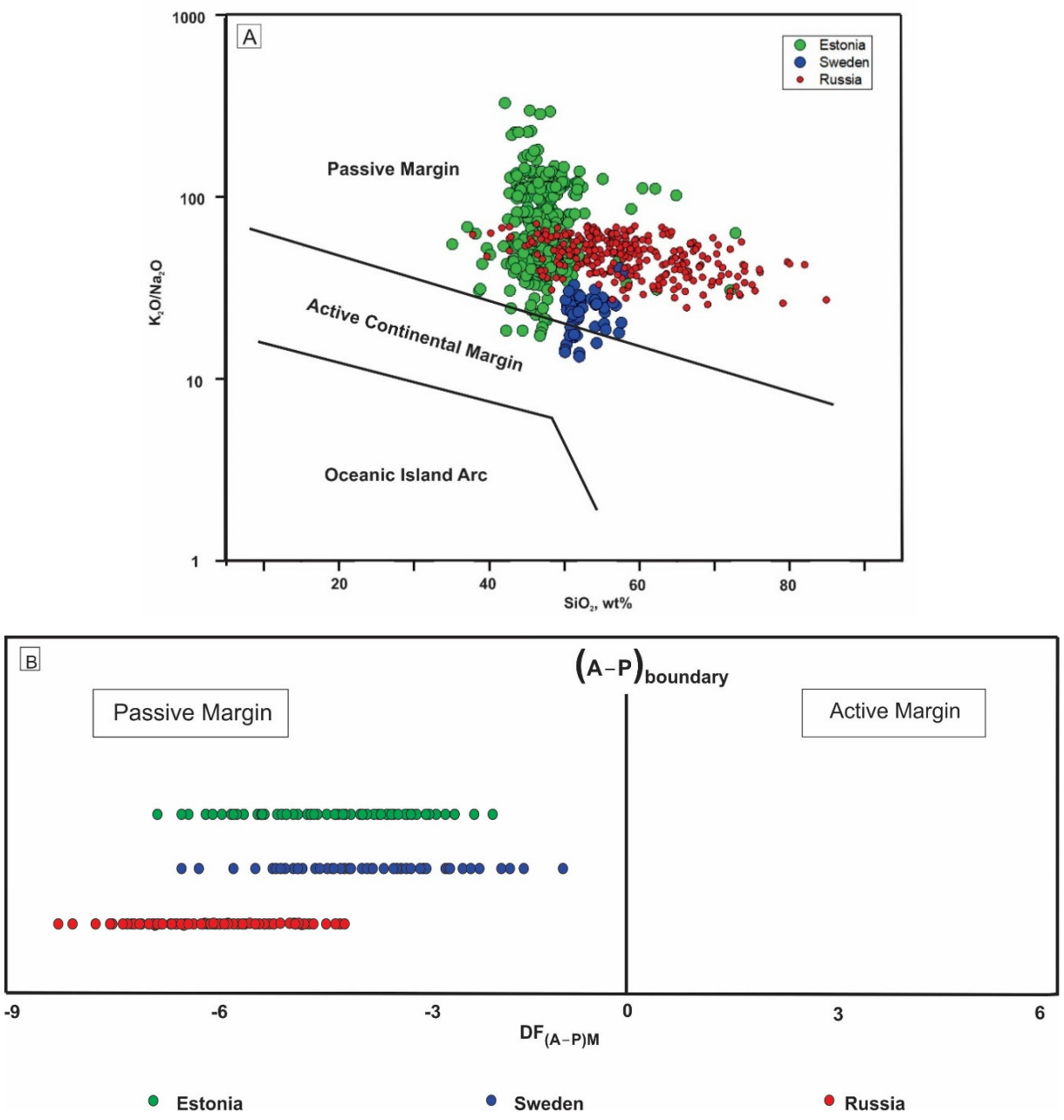

Figure 5. Tectonic setting discrimination plot for the studied black shales: (**A**) K_2O/Na_2O versus SiO_2 [3]; (**B**) major element-based active and passive margin setting discrimination model [7]. The black vertical line in figure (**B**) represents the boundary between active margin (right) and passive margin (left) fields. For steps to calculate $DF_{(A-P)M}$, see [7].

A new method of discriminating tectonic settings proposed by Verma and Armstrong-Altrin [7] is also employed in this study to infer the tectonic setting of the Baltoscandian black shales (Figure 5B). This method uses either major element (SiO_2 to P_2O_5) data only, or a combination of major and trace elements (Cr, Nb, Ni, V, Y and Zr) with the application of the computer software "APMdisc". It has been demonstrated that this approach may have great success in accurately discriminating active and passive margin tectonic settings [7,56,57]. In this paper, major element data of the black shale samples

were used to infer the tectonic settings of the studied sites. The samples plot in the passive margin field of this discriminant (with over 99% confidence rate for all samples), suggesting a passive margin setting for the Baltoscandian black shales (Figure 5B). This interpretation agrees well with an earlier interpretation based on the Roser and Korsch [3] discriminant model and with general knowledge of Baltoscandian geotectonic settings during the Lower Paleozoic era [30].

5.3. Paleoweathering

The degree of weathering has been inferred using the Chemical Index of Alteration, CIA, given as CIA = [Al_2O_3/(Al_2O_3 + CaO* + Na_2O + K_2O)] × 100 [58]. All values in the above equation are in molar proportions, whereas CaO* represents the amount of CaO incorporated into the silicate fraction of the rock.

The CIA values of the studied black shales range from 53 to 80 (Figure 6). Samples from Sweden have the highest CIA values of 61–80, whereas samples from Estonia and Russia are similar, in the range of 54–64 and 53–63, respectively.

The significant difference between the CIA values of samples from Sweden and those from Estonia and Russia could be related to factors such as variation in the dominant lithology of terrigenous provenance areas, an increase in compositional maturity during sediment transport [15,59], and/or addition of cations by marine reverse weathering reactions [60], or by late diagenetic basinal brines [61].

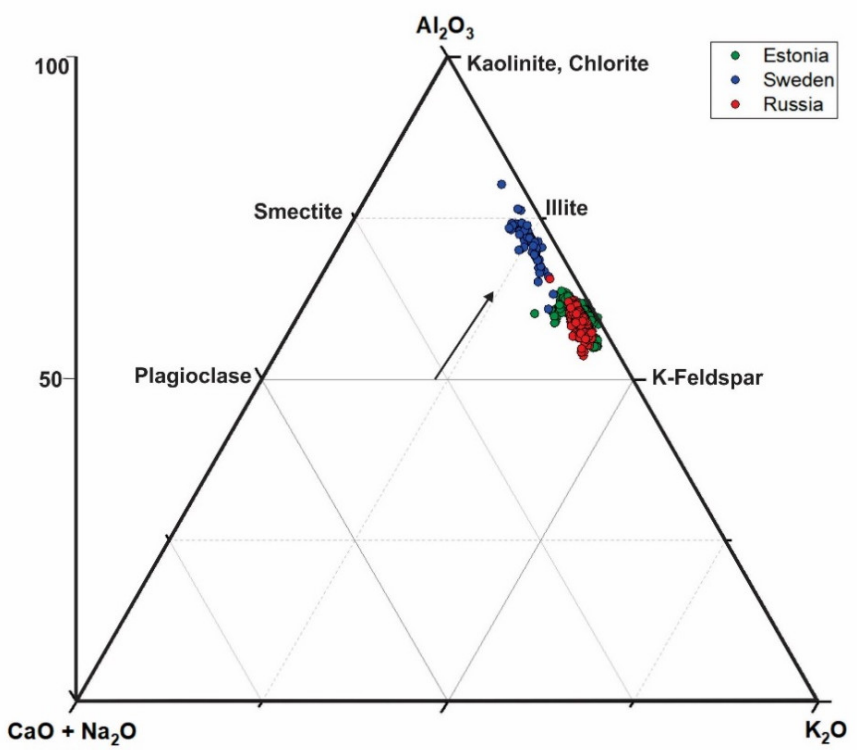

Figure 6. Ternary diagram for the estimation of the degree of chemical weathering of the black shales, based on molecular proportions of Al_2O_3, CaO, Na_2O, and K_2O [61]. Vertical scale represents the Chemical Index of Alteration.

On the geochemical ternary plot (Figure 6), the samples show a trend along the Al_2O_3–K_2O compositional line, which represents an advanced stage of weathering. Samples from Russia and Estonia cluster just above the K-feldspar region, whereas samples from Sweden cluster around illite.

The scattered nature of the points (points not falling on a pre-defined weathering trend) indicates that secondary processes may have resulted in the redistribution of potassium in the silicate fraction [46]. It is therefore difficult to estimate concrete weathering profiles;

however, based on the provenance interpretation in [62], the most likely profile would be somewhere near intermediate to felsic rock composition (indicated by an arrow in Figure 6). If this is the case, the studied black shale samples, especially those from Russia and Estonia, have experienced significant potassium enrichment resulting in lower CIA values as defined by Fedo et al. [63].

It is a common practice to evaluate the degree of weathering using the Chemical Index of Weathering (CIW) [64] method, where potassium alteration is believed to affect weathering interpretations from the CIA method [65–67]. The CIW is calculated as follows:

$$CIW = [A1_2O_3/(AI_2O_3 + CaO + Na_2O)] \times 100 \text{ (in molecular proportions).}$$

The average CIW values of samples from Estonia, Sweden, and Russia are similar, at 97, 96, and 95, respectively, thus indicating an intense degree of weathering of the source material.

This is a strong indication that secondary K-enrichment has overprinted the CIA values of the primary mineral matter. A high degree of weathering is expected in the Baltoscandian black shales, because temperatures were high during the Tremadocian stage when the black shale formed [33]. Nevertheless, the source and timing of possible secondary K-enrichment remain elusive. Some previous studies have suggested a significant input of volcanic ash to the regional sedimentary budget of the paleobasin [68–70] which could account for potassium enrichment in the considered black shale [69]. Indeed, similar potassium enrichment, together with the widespread formation of authigenic low sanidine and illitic illite-smectite, is also known as being from the Lower Paleozoic bentonites of Estonia. Mass balance calculations suggest that a considerable amount of potassium was added during the alteration of primary ash to bentonite assemblages. The major source of extra potassium could have been late diagenetic K-rich fluids driven by the development of the Scandinavian Caledonides [71]; however, it is also important to add that large areas of felsic high potassium granitoids and granitic gneisses occur in Southern and Central Finland. The physical and chemical erosional products of that material may well be contributing to potassium enrichment in the studied black shales.

6. Conclusions

The Lower Paleozoic black shales of Estonia, Sweden and Russia are highly enriched in a variety of trace elements (U, V, Mo, and Pb (except in Swedish samples)), slightly enriched in SiO_2, Fe_2O_3, K_2O, and TiO_2, and highly depleted in CaO, Na_2O, and MnO, relative to average shales (PAAS).

Major and trace element ratios and discriminant plots suggest that the initial material of the black shale was generally derived from intermediate to felsic rocks and recycled sediments.

Tectonic setting discriminant plots suggest a passive margin setting for the studied Lower Paleozoic black shales.

The CIW values suggest intense degree of chemical weathering of the clastic material of the black shale. The CIA values may not accurately reflect the degree of weathering of the Baltoscandian shales as the shale may have experienced significant secondary potassium enrichment during diagenesis.

Supplementary Materials: The following supporting information can be downloaded at: https://www.mdpi.com/article/10.3390/min12050602/s1, Table S1: Major (wt%) and trace (ppm) element concentrations of studied black shale drill cores in Estonia and Russia, and outcrops in Sweden.

Author Contributions: Conceptualization, S.O., A.S. and E.G.P.; Data curation, A.S. and E.G.P.; Methodology, S.O., A.S., E.G.P. and R.H.; Software, S.O. and S.H.; Supervision, A.S. and L.A.; Visualization, S.O. and S.H.; Writing—original draft, S.O.; Writing—review and editing, S.O., A.S., E.G.P., R.H., S.H. and L.A. All authors have read and agreed to the published version of the manuscript.

Funding: This study was supported by the Estonian Science Agency project RESTA18 and Estonian Centre of Analytical Chemistry.

Data Availability Statement: Data are contained within the Supplementary Materials.

Conflicts of Interest: The authors declare no conflict of interest.

References

1. Bhatia, M.R.; Crook, A.W. Trace element characteristics of graywackes and tectonic setting discrimination of sedimentary basins. *Contr. Min. Pet.* **1986**, *92*, 181–193. [CrossRef]
2. Hayashi, K.; Fujisawa, H.; Holland, H.D.; Ohmoto, H. Geochemistry of 1.9 Ga sedimentary rocks from northeastern Labrador, Canada. *Geochim. Cosmochim. Acta* **1997**, *61*, 4115–4137. [CrossRef]
3. Roser, B.P.; Korsch, R.J. Determination of tectonic setting of sandstone-mudstone suites using SiO_2 content and K_2O/Na_2O ratio. *J. Geol.* **1986**, *94*, 635–650. [CrossRef]
4. Roser, B.P.; Korsch, R.J. Provenance signatures of sandstone mudstone suites determined using discriminant function analysis of major-element data. *Chem. Geol.* **1988**, *67*, 119–139. [CrossRef]
5. Cullers, R.L. The geochemistry of shales, siltstones and sandstones of Pennsylvanian–Permian age, Colorado, USA: Implications for provenance and metamorphic studies. *Lithos* **2000**, *51*, 181–203. [CrossRef]
6. Armstrong-Altrin, J.S.; Lee, Y.I.; Verma, S.P.; Ramasamy, S. Geochemistry of sandstones from the upper Miocene Kudankulam formation, southern India: Implications for provenance, weathering, and tectonic setting. *J. Sediment. Res.* **2004**, *74*, 285–297. [CrossRef]
7. Verma, S.P.; Armstrong-Altrin, J.S. Geochemical discrimination of siliciclastic sediments from active and passive margin settings. *Sediment. Geol.* **2016**, *332*, 1–12. [CrossRef]
8. Zhao, J.; Jin, Z.; Jin, Z.; Geng, Y.; Wen, X.; Yan, C. Applying sedimentary geochemical proxies for paleoenvironment interpretation of organic-rich shale deposition in the Sichuan Basin, China. *Int. J. Coal Geol.* **2016**, *163*, 52–71. [CrossRef]
9. Mitra, R.; Chakrabarti, G.; Shome, D. Geochemistry of the Palaeo–Mesoproterozoic Tadpatri shales, Cuddapah basin, India: Implications on provenance, paleoweathering and paleoredox conditions. *Acta. Geochim.* **2018**, *37*, 715–733. [CrossRef]
10. Ofili, S.; Soesoo, A. General geology and geochemistry of the Lokpanta formation oil shale, Nigeria. *Oil Shale* **2021**, *38*, 1–25. [CrossRef]
11. Calvert, S.E.; Pederson, T.F. Geochemistry of recent oxic and anoxic marine sediments: Implications for the geological record. *Mar. Geol.* **1993**, *113*, 67–88. [CrossRef]
12. Crombez, V.; Rohais, S.; Euzen, T.; Riquier, L.; Baudin, F.; Hernandez-Bilbao, E. Trace metal elements as paleoenvironmental proxies: Why should we account for sedimentation rate variations? *Geology* **2020**, *48*, 839–843. [CrossRef]
13. Schovsbo, N.H. Why barren intervals? A taphonomic case study of the Scandinavian Alum Shale and its faunas. *Lethaia* **2001**, *34*, 271–285. [CrossRef]
14. Armands, G. Geochemical studies of uranium, molybdenium and vanadium in a Swedish alum shale. *Stockh. Univ. Contr. Geol.* **1972**, *21*, 148.
15. Pukkonen, E.; Rammo, M. Distribution of molybdenum and uranium in the Tremadoc Graptolite Argillite (Dictyonema Shale) of north-western Estonia. *Bull. Geol. Surv. Estonia* **1992**, *2*, 3–15.
16. Schovsbo, N.H. Uranium enrichment shorewards in black shales: A case study from the Scandinavian Alum Shale. *GFF* **2002**, *124*, 107–115. [CrossRef]
17. Gill, B.C.; Lyons, T.W.; Young, S.A.; Kump, L.R.; Knoll, A.H.; Saltzman, M.R. Geochemical evidence for widespread euxinia in the later Cambrian Ocean. *Nature* **2011**, *469*, 80–83. [CrossRef]
18. Voolma, M.; Soesoo, A.; Hade, S.; Hints, R.; Kallaste, T. Geochemical heterogeneity of the Estonian graptolite argillite. *Oil Shale* **2013**, *30*, 377–401. [CrossRef]
19. Lecomte, A.; Cathelineau, M.; Michels, R.; Peiffert, C.; Brouand, M. Uranium mineralization in the Alum Shale Formation (Sweden): Evolution of a U-rich marine black shale from sedimentation to metamorphism. *Ore Geol. Rev.* **2017**, *88*, 71–98. [CrossRef]
20. Yang, S.; Schulz, H.M.; Schovsbo, N.; Mayanna, S. The organic geochemistry of "Kolm", a unique analogue for the understanding of molecular changes after significant uranium irradiation. *Int. J. Coal Geol.* **2019**, *209*, 89–93. [CrossRef]
21. Schovsbo, N.H.; Nielsen, A.T.; Harstad, A.O.; Bruton, D.L. Stratigraphy and geochemical composition of the Cambrian Alum Shale Formation in the Porsgrunn core, Skien-Langesund district, southern Norway. *Bull. Geol. Soc. Den.* **2018**, *66*, 1–20. [CrossRef]
22. Schulz, H.M.; Yang, S.; Schovsbo, N.H.; Rybacki, E.; Ghanizadeh, A.; Bernard, S.; Mahlstedt, N.; Krüger, M.; Amann-Hildebrandt, A.; Krooss, B.M.; et al. The Furongian to lower Ordovician alum shale formation in conventional and unconventional petroleum systems in the Baltic Basin—A review. *Earth-Sci. Rev.* **2021**, *218*, 103674. [CrossRef]
23. Vyalov, V.I.; Bogomolov, A.K.; Mikhailov, V.A. The uranium content in Dictyonema shale of the Kaibolovo–Gostilitsy area in the Baltic basin (Leningrad region). *Mosc. Univ. Geol. Bull.* **2017**, *72*, 326–331. [CrossRef]
24. Hade, S.; Soesoo, A. Estonian graptolite argillites revisited: A future resource? *Oil Shale* **2014**, *31*, 4–18. [CrossRef]
25. Utsal, K.; Kivimägi, E.; Utsal, V. About the method of investigating Estonian graptolithic argillite and its mineralogy. *Tartu Riikliku Ülik. Toim.* **1980**, *527*, 116–138.
26. Kleesment, A.; Kurvits, T. Mineralogy of Tremadoc graptolitic argillites of North Estonia. *Oil Shale* **1987**, *4*, 130–139.

27. Artyushkov, E.A.; Lindström, M.; Popov, L.E. Relative sea-level changes in Baltoscandia in the Cumbrian and early Ordovician: The predominance of tectonic factors and the absence of large scale eustatic fluctuations. *Tectonophysics* **2000**, *320*, 375–407. [CrossRef]
28. Sturesson, U.L.F.; Popov, L.E.; Holmer, L.E.; Bassett, M.G.; Felitsyn, S.; Belyatsky, B. Neodymium isotopic composition of Cambrian–Ordovician biogenic apatite in the Baltoscandian Basin: Implications for palaeogeographical evolution and patterns of biodiversity. *Geol. Mag* **2005**, *142*, 419–439. [CrossRef]
29. Schulz, H.M.; Yang, S.; Panova, E.; Bechtel, A. The role of Pleistocene meltwater-controlled uranium leaching in assessing irradiation-induced alteration of organic matter and petroleum potential in the Tremadocian Koporie Formation (Western Russia). *Geochim. Cosmochim. Acta* **2019**, *245*, 133–153. [CrossRef]
30. Cocks, L.R.M.; Torsvik, T.H. Baltica from the late Precambrian to mid-Palaeozoic times: The gain and loss of a terrane's identity. *Earth Sci. Rev.* **2005**, *72*, 39–66. [CrossRef]
31. Nielsen, A.T.; Schovsbo, N.H. Cambrian to basal Ordovician lithostratigraphy in Southern Scandinavia. *Bul. Geol. Soc. Den.* **2006**, *53*, 47–92.
32. Babcock, L.E.; Peng, S.C.; Brett, C.E.; Zhu, M.Y.; Ahlberg, P.; Bevis, M.; Robison, R.A. Global climate, sea level cycles, and biotic events in the Cambrian Period. *Palaeoworld* **2015**, *24*, 5–15. [CrossRef]
33. Trotter, J.A.; Williams, I.S.; Barnes, C.R.; Lécuyer, C.; Nicoll, R.S. Did cooling oceans trigger Ordovician biodiversification? Evidence from conodont thermometry. *Science* **2008**, *321*, 550–554. [PubMed]
34. Popov, L.E.; Álvaro, J.J.; Holmer, L.E.; Bauert, H.; Ghobadi Pour, M.; Dronov, A.V.; Lehnert, O.; Hints, O.; Männik, P.; Zhang, Z.; et al. Glendonite occurrences in the Tremadocian of Baltica: First early Palaeozoic evidence of massive ikaite precipitation at temperate latitudes. *Sci. Rep.* **2019**, *9*, 7205.
35. Männil, R. Evolution of the Baltic Basin during the Ordovician. *Valgus Tallinn* **1966**, *248*, 200, (In Russian with English summary).
36. Kaljo, D.; Kivimagi, E. On the distribution of graptolites in the Dictyonema shale of Estonia and the uncontemporaneity of its different facies. *Proc. Acad. Sci. Estonian Chem. Geol.* **1970**, *19*, 334–341.
37. Heinsalu, H.; Kaljo, D.; Kurvits, T.; Viira, V. The stratotype of the Orasoja member (Tremadocian, Northeast Estonia): Lithology, mineralogy, and biostratigraphy. *Proc. Estonian Acad. Sci. Geol.* **2003**, *52*, 135–154.
38. Buchardt, B.; Nielsen, A.T.; Schovsbo, N.H. Alun skiferen i Skandinavien. *Geol. Tidskift* **1997**, *3*, 1–30.
39. Nielsen, A.T.; Schovsbo, N.H. The lower Cambrian of Scandinavia: Depositional environment, sequence stratigraphy and palaeogeography. *Earth-Sci. Rev.* **2011**, *107*, 207–310.
40. Nikishin, A.M.; Ziegler, P.A.; Stephenson, R.A.; Cloetingh, S.A.P.L.; Furne, A.V.; Fokin, P.A.; Ershov, A.V.; Bolotov, S.N.; Korotaev, M.V.; Alekseev, A.S.; et al. Late Precambrian to Triassic history of the East European Craton: Dynamics of sedimentary basin evolution. *Tectonophysics* **1996**, *268*, 23–63. [CrossRef]
41. Puura, E.; Neretnieks, I.; Kirsimäe, K. Atmospheric oxidation of the pyritic waste rock in Maardu, Estonia. 1 field study and modelling. *Environ. Geol.* **1999**, *39*, 1–19.
42. Vind, J.; Bauert, H. *Geochemical Characterization of the Tremadocian Black Shale in North-Western Estonia, EGF9330*; Geological Survey of Estonia: Rakvere, Estonia, 2020.
43. Soesoo, A.; Vind, J.; Hade, S. Uranium and thorium resources of Estonia. *Minerals* **2020**, *10*, 798.
44. Vyalov, V.I.; Volkova, G.M.; Balakhonova, A.S. Report: Prospecting for rhenium in dictionem shales and phosphorites of the Baltic basin on the Kaibolovo-Gostilitskaya area with an assessment of the forecast rhenium resources by categories P2-P1. In *Books 1–4*; VSEGEI: St. Petersburg, Russia, 2014; book 1-120 s., book 2-112 s., book 3-123., book 4-122 s.
45. Taylor, S.R.; McLennan, S.M. *The Continental Crust: Its Composition and Evolution*; Blackwell: Oxford, UK, 1985; Volume 312.
46. McLennan, S.M.; Hemming, S.R.; McDanniel, D.K.; Hanson, G.N. Geochemical approaches to sedimentation, provenance, and tectonic. *Geol. Soc. Am. Spec.* **1993**, *284*, 21–40.
47. Blatt, H. Provenance determinations and recycling of sediments. *J. Sediment. Res.* **1967**, *37*, 1031–1044.
48. Cullers, R.L.; Berendsen, P. The provenance and chemical variation of sandstones associated with the Mid-continent Rift System, USA. *Eur. J. Miner.* **1998**, *10*, 987–1002. [CrossRef]
49. Dronov, A.; Tolmacheva, T.; Raevskaya, E.; Nestell, M. Cambrian and Ordovician of St.Petersburg region. In Proceedings of the 6th Baltic Stratigraphical Conference IGCP 503 Meeting, St. Petersburg, Russia, 23–25 August 2005. Guidebook of the Pre-Conference Field Trip.
50. Dronov, A.V.; Ainsaar, L.; Kaljo, D.; Meidla, T.; Saadre, T.; Einasto, R. Ordovician of Baltoscandia: Facies, sequences and sea-level changes. *Ordovician World* **2011**, *14*, 143–150.
51. Dahl, T.W.; Siggaard-Andersen, M.L.; Schovsbo, N.H.; Persson, D.O.; Husted, S.; Hougård, I.W.; Dickson, A.J.; Kjær, K.; Nielsen, A.T. Brief oxygenation events in locally anoxic oceans during the Cambrian solves the animal breathing paradox. *Sci. Rep.* **2019**, *9*, 1–9.
52. Penny, A.M.; Hints, O.; Kröger, B. Carbonate shelf development and early Paleozoic benthic diversity in Baltica: A hierarchical diversity partitioning approach using brachiopod data. *Paleobiology* **2021**, *48*, 1–21.
53. Mikkola, P.; Heilimo, E.; Luukas, J.; Kousa, J.; Aatos, S.; Makkonen, H.; Niemi, S.; Nousiainen, M.; Ahven, M.; Romu, I.; et al. Geological evolution and structure along the southeastern border of the Central Finland Granitoid Complex. *Geol. Surv. Finl. Bull.* **2018**, *407*, 5–27.

54. Alvarez, N.C.; Roser, B.P. Geochemistry of black shales from the Lower Cretaceous Paja formation, Eastern Cordillera, Colombia: Source weathering, provenance, and tectonic setting. *J. S. Am. Earth Sci.* **2007**, *23*, 271–289.
55. Liu, B.; Song, Y.; Zhu, K.; Su, P.; Ye, X.; Zhao, W. Mineralogy and element geochemistry of salinized lacustrine organic-rich shale in the Middle Permian Santanghu Basin: Implications for paleoenvironment, provenance, tectonic setting and shale oil potential. *Mar. Pet. Geol.* **2020**, *120*, 104569. [CrossRef]
56. Ivančič, K. Provenance of the Miocene Slovenj Gradec Basin sedimentary fill, Western Central Paratethys. *Sediment. Geol.* **2018**, *375*, 256–267. [CrossRef]
57. Deng, T.; Li, Y.; Wang, Z.J.; Yu, Q.; Dong, S.L.; Yan, L.; Hu, W.C.; Chen, B. Geochemical characteristics and organic matter enrichment mechanism of black shale in the Upper Triassic Xujiahe Formation in the Sichuan basin: Implications for paleoweathering, provenance and tectonic setting. *Mar. Petrol. Geol.* **2019**, *109*, 698–716. [CrossRef]
58. Nesbitt, H.W.; Young, G.M. Formation and diagenesis of weathering profiles. *J. Geol.* **1989**, *97*, 129–147. [CrossRef]
59. Schovsbo, N.H. The geochemistry of Lower Palaeozoic sediments deposited on the margins of Baltica. *Bull. Geol. Soc. Den.* **2003**, *50*, 11–27. [CrossRef]
60. Michalopoulos, P.; Aller, R.C.; Reeder, R.J. Conversion of diatoms to clays during early diagenesis in tropical, continental shelf muds. *Geology* **2000**, *28*, 1095–1098. [CrossRef]
61. Hearn, P.P., Jr.; Sutter, J.F.; Belkin, H.E. Evidence for Late-Paleozoic brine migration in Cambrian carbonate rocks of the central and southern Appalachians: Implications for Mississippi Valley-type sulfide mineralization. *Geochim. Cosmochim. Acta* **1987**, *51*, 1323–1334. [CrossRef]
62. Nesbitt, H.W.; Young, G.M. Prediction of some weathering trends of plutonic and volcanic rocks based on thermodynamic and kinetic considerations. *Geochim. Cosmochim. Acta* **1984**, *48*, 1523–1534. [CrossRef]
63. Fedo, C.M.; Nesbitt, H.W.; Young, G.M. Unravelling the effects of potassium metasomatism in sedimentary rocks and paleosols, with implications for paleoweathering conditions and provenance. *Geology* **1995**, *23*, 921–924. [CrossRef]
64. Harnois, L. The CIW index: A new chemical index of weathering. *Sediment. Geol.* **1988**, *55*, 319–322. [CrossRef]
65. Condie, K.C.; Boryta, M.D.; Liu, J.; Qian, X. The origin of khondalites: Geochemical evidence from the Archean to early Proterozoic granulite belt in the North China craton. *Precambrian Res.* **1992**, *59*, 207–223. [CrossRef]
66. Maynard, J.B. Chemistry of modern soils as a guide to interpreting Precambrian paleosols. *J. Geol.* **1992**, *100*, 279–289. [CrossRef]
67. Condie, K.C. Chemical composition and evolution of the upper continental crust: Contrasting results from surface samples and shales. *Chem. Geol.* **1993**, *104*, 1–37. [CrossRef]
68. Lindgreen, H.; Drits, V.A.; Sakharov, B.A.; Salyn, A.L.; Wrang, P.; Dainyak, L.G. Illite-smectite structural changes during metamorphism in black Cambrian Alum shales from the Baltic area. *Am. Miner.* **2000**, *85*, 1223–1238. [CrossRef]
69. Kiipli, T.; Soesoo, A.; Kallaste, T. Geochemical evolution of Caledonian volcanism recorded in the sedimentary rocks of the eastern Baltic region. *Geol. Soc. Lond. Spec. Pub.* **2014**, *390*, 177–192. [CrossRef]
70. Kiipli, T.; Dahlquist, P.; Kallaste, T.; Kiipli, E.; Nolvak, J. Upper Katian (Ordovician) bentonites in the East Baltic, Scandinavia and Scotland: Geochemical correlation and volcanic source interpretation. *Geol. Mag.* **2015**, *152*, 589–602. [CrossRef]
71. Somelar, P.; Kirsimäe, K.; Hints, R.; Kirs, J. Illitization of Early Paleozoic K-bentonites in the Baltic Basin: Decoupling of burial-and fluid-driven processes. *Clay Miner.* **2010**, *58*, 388–398. [CrossRef]